Title

Differences in codon bias and GC content contribute to the balanced expression of TLR7 and TLR9

Journal

Proceedings of the National Academy of Sciences of the United States of America, 113(10)

ISSN

0027-8424

Authors

Newman, Zachary R
Young, Janet M
Ingolia, Nicholas T
et al.

Publication Date

2016-03-08

DOI

10.1073/pnas.1518976113

Peer reviewed

Differences in codon bias and GC content contribute to the balanced expression of TLR7 and TLR9

Zachary R. Newman[a], Janet M. Young[b], Nicholas T. Ingolia[c], and Gregory M. Barton[a,1]

[a]Division of Immunology and Pathogenesis, Department of Molecular and Cell Biology, University of California, Berkeley, CA 94720; [b]Division of Basic Sciences, Fred Hutchinson Cancer Research Center, Seattle, WA 98109; and [c]Division of Biochemistry, Biophysics and Structural Biology, Department of Molecular and Cell Biology, University of California, Berkeley, CA 94720

Edited by Ruslan Medzhitov, Yale University School of Medicine, New Haven, CT, and approved January 26, 2016 (received for review September 25, 2015)

The innate immune system detects diverse microbial species with a limited repertoire of immune receptors that recognize nucleic acids. The cost of this immune surveillance strategy is the potential for inappropriate recognition of self-derived nucleic acids and subsequent autoimmune disease. The relative expression of two closely related receptors, Toll-like receptor (TLR) 7 and TLR9, is balanced to allow recognition of microbial nucleic acids while limiting recognition of self-derived nucleic acids. Situations that tilt this balance toward TLR7 promote inappropriate responses, including autoimmunity; therefore, tight control of expression is critical for proper homeostasis. Here we report that differences in codon bias limit TLR7 expression relative to TLR9. Codon optimization of *Tlr7* increases protein levels as well as responses to ligands, but, unexpectedly, these changes only modestly affect translation. Instead, we find that much of the benefit attributed to codon optimization is actually the result of enhanced transcription. Our findings, together with other recent examples, challenge the dogma that codon optimization primarily increases translation. We propose that suboptimal codon bias, which correlates with low guanine-cytosine (GC) content, limits transcription of certain genes. This mechanism may establish low levels of proteins whose overexpression leads to particularly deleterious effects, such as TLR7.

Toll-like receptors | codon bias | GC content | TLR7 | TLR9

Toll-like receptors (TLRs) recognize broadly conserved microbial features and initiate downstream signaling events critical for proper responses to infection, including production of key cytokines and initiation of the secondary immune response. Nearly half of these TLRs (TLR3, TLR7, TLR8, TLR9, and TLR13) recognize nucleic acid ligands. Although these nucleic acid-sensing TLRs detect features generally associated with viruses and bacteria, the potential exists for recognition of self-derived nucleic acid ligands. This self-recognition has been proposed to lead to failures in self-tolerance that promote autoimmune diseases such as systemic lupus erythematosus (SLE) and rheumatoid arthritis, particularly in driving the production of autoantibodies against nucleic acid and nucleic acid-containing complexes (1). This trade-off exemplifies the balance that must be struck between a proper response to infection and the avoidance of improper activation against self.

The closely related nucleic acid-sensing receptors TLR7 and TLR9, whose ligands are ssRNA and DNA with unmethylated CpG motifs, respectively, are regulated at several distinct mechanistic levels (2). At the transcriptional level, *Tlr7* and *Tlr9* expression is restricted to relatively few immune cell types in mice. Interestingly, in humans their expression is limited even further (3). The activation of both TLR7 and TLR9 is limited to endolysosomal compartments, a location considered largely devoid of self-nucleic acid, through restricted cellular localization and a requirement for pH-dependent receptor processing (4). Thus, multiple mechanisms serve to limit TLR7 and TLR9 signaling.

Despite the similarities in the regulation of TLR7 and TLR9, more recent studies have revealed differences between the two receptors. Although both traffic to endosomes, each receptor is sorted via distinct trafficking routes (5, 6). Furthermore, TLR7 and TLR9 have been shown to compete with each other for the factors required for signaling in an in vitro setting (7). It also is possible that interplay with other TLRs can influence TLR7 and TLR9 responses (8). A point mutation in the trafficking chaperone *Unc93b1* biases signaling toward TLR7 at the expense of TLR9 (9). Type I interferons, cytokines strongly linked to autoimmune diseases such as SLE (10), have been shown to regulate the expression of TLR7 and TLR9 differentially in B cells (11). Thus, although the detrimental effects of dysregulated nucleic acid-sensing TLRs have been appreciated for some time, there is accumulating evidence that TLR7 and TLR9 functions are controlled by distinct regulatory mechanisms.

The critical need to regulate nucleic acid-sensing TLRs, especially TLR7, in vivo is exemplified by mouse models of SLE. Both TLR7 and TLR9 promote autoantibody production in these models (12–14); however, these receptors play opposing roles in overall disease progression. Although the lack of TLR7 is protective in these models, TLR9 deficiency paradoxically exacerbates disease in a TLR7-dependent fashion (15, 16). It has been suggested that the lack of TLR9 disrupts the balance of TLR7 responses in these models; however, it remains unclear why TLR7 is more prone to dysregulation. Importantly, an intrinsic role for TLR7 in autoimmunity has been described, because disease is triggered by the introduction of additional copies of *Tlr7* (17). Interestingly, this study also found that varying levels of *Tlr7* gene dosage leads to different autoimmune diseases, with phenotypic outcomes ranging from SLE-like disease to acute inflammation. These results imply that different regulatory barriers are overcome as the amount of TLR7 protein

Significance

Codon bias, the unequal use of synonymous codons to encode amino acids, is known to influence protein expression. Our work finds that codon bias can limit the expression of Toll-like receptor 7, a receptor implicated in autoimmune diseases such as lupus. Surprisingly, we find that the improved protein production associated with codon optimization is not caused by increased translation but instead is caused by an increased rate of transcription. We attribute this change in transcription to increased guanine-cytosine (GC) content following codon optimization. Thus, our work not only addresses a fundamental aspect of immune regulation but also provides mechanistic insight into the controversial issue of how codon bias and GC content influence protein expression.

Author contributions: Z.R.N. and G.M.B. designed research; Z.R.N. performed research; J.M.Y. and N.T.I. contributed new reagents/analytic tools; Z.R.N., J.M.Y., N.T.I., and G.M.B. analyzed data; and Z.R.N., J.M.Y., N.T.I., and G.M.B. wrote the paper.

The authors declare no conflict of interest.

This article is a PNAS Direct Submission.

[1]To whom correspondence should be addressed. Email: barton@berkeley.edu.

This article contains supporting information online at www.pnas.org/lookup/suppl/doi:10.1073/pnas.1518976113/-/DCSupplemental.

increases. Limiting TLR7 expression also has been shown to be important in human disease, because copy number variations of *TLR7* are sometimes seen in patients with SLE (18), and a point mutation in the 3′ UTR of *TLR7* correlates with increased *TLR7* mRNA levels (19). Additionally, the point mutation discovered in the chaperone *Unc93b1*, which biases signaling toward TLR7 and away from TLR9, promotes autoimmunity in mice (9). Regulation of TLR7 and TLR9 protein levels therefore is critical for the balance between protective immunity and autoimmunity. Further elucidation of the mechanisms maintaining this balance will be important to understand better how perturbation of the system results in autoimmunity.

In this study, we identify differences in codon bias between *Tlr7* and *Tlr9* and explore how these differences influence protein abundance. The mechanism by which codon bias—the unequal use of synonymous codons encoding for a given amino acid—impacts translation efficiency remains a hotly debated subject (20, 21). Recent advances in technology and experimental design, in particular ribosome profiling (22), have allowed researchers to explore mechanisms related to codon bias and protein expression on a global scale. Nonetheless, disagreement persists, and conclusions about the role of codon bias seem heavily influenced by the method of analysis used (23–25). On a smaller scale, optimizing codons of individual proteins can lead to increased protein expression, but the mechanism(s) underlying the increased protein remains controversial. Several groups have reported that the protein increase results from an increase in the rate of translation (26, 27), whereas others have observed an increase in the rate of transcription (28, 29). Furthermore, a recent study concluded that, although transcriptional control is the broadest means of controlling protein expression, a fraction of proteins are differentially regulated at the translational level (30). However, investigators, have tended to focus on extreme examples, either by comparisons with fully optimized sequences or by limiting global analysis to genes that meet certain thresholds. Absent are more nuanced comparisons that carefully investigate how codon bias fine-tunes the various mechanisms involved in protein expression, particularly of proteins for which the dysregulation of expression has clear biological significance.

Here we show that codon bias can play a crucial role in setting protein levels of TLR7 and TLR9. Additionally we are able to elucidate and, importantly, separate the multiple mechanistic contributions of codon bias that converge to limit TLR7 but not TLR9 protein expression. Unexpectedly, we find that the impact of codon bias on protein levels is mediated largely through transcription rather than translation.

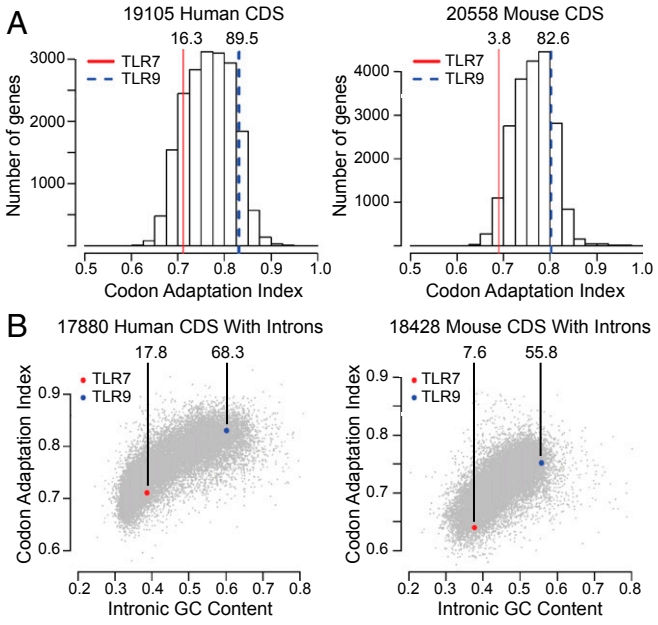

C

Frequency of Leu Codons (%)

	TLR7	TLR9	GenomeAvg
CTG	18.6%	56.0%	39.6%
TTA	14.4%	0.5%	7.5%
TTG	19.8%	7.3%	12.5%
CTT	18.6%	5.8%	13.0%
CTA	10.2%	8.4%	7.2%
CTC	18.6%	22.0%	20.0%

Total Leu Codons

	TLR7	TLR9
CTG	31	107
TTA	24	1
TTG	33	14
CTT	31	11
CTA	17	16
CTC	31	42
Total	167	191

Fig. 1. *Tlr7* and *Tlr9* have distinct codon biases. (*A*) *Tlr7* and *Tlr9* differ in their use of optimal codons. Histograms display the calculated CAI for all CDS in humans and mice, with *Tlr7* (red) and *Tlr9* (blue) highlighted along with their CAI percentiles. (*B*) Codon optimization correlates with GC content. The CAI is plotted against the intronic GC content for all human and mouse CDS. CAI percentiles compared with genes within 2.5% GC of both *Tlr7* and *Tlr9* are indicated. (*C*) The frequency of codons encoding for the amino acid leucine differs in murine *Tlr7* and *Tlr9*. The frequency (*Left*) and absolute number (*Right*) of leucine-encoding codons for murine TLR7 and TLR9 are shown. The optimal codon CTG (green), the suboptimal codon TTA (red), and other leucine codons displaying a bias (gray) are highlighted.

Results

***Tlr7* and *Tlr9* Have Distinct Codon Biases.** A previous study suggested that codon bias may be important for the expression of TLRs, noting that *Tlr7* uses a high percentage of infrequent codons, whereas *Tlr9* uses more common codons (31). We also have reported that codon optimization of *Tlr7* dramatically increases protein levels in an in vitro setting, whereas *Tlr9* required no such optimization (6). However, these studies did not elucidate the mechanisms responsible for the increase in protein, nor did they address the biological significance of potential differences in translation. Because of the clear link between increased TLR7 levels and autoimmune disease, we sought to investigate whether codon bias limits TLR7 responses and the mechanisms underlying such potential regulation.

We performed codon use analysis of the *Tlr7* and *Tlr9* genes in mice and humans. Using the codon adaptation index (CAI) as a measure of bias, we compared *Tlr7* and *Tlr9* coding sequences (CDS) to all mouse and human CDS (Fig. 1*A*). We chose to use the CAI as our measure because it is designed to be predictive of protein expression (32). Relative to all mouse and human genes, *Tlr7* scored in the third and 17th percentiles, respectively, whereas *Tlr9* scored in the 82nd and 89th percentiles. Therefore, *Tlr7* and *Tlr9* fell on opposite ends of the distribution of genes scored for use of optimal codons.

More frequently used codons in mice and humans correlate with a higher guanine-cytosine (GC) content, and genes reflect the GC content of their chromosomal context (21). Accordingly, we sought to find out whether the codon bias we observed for *Tlr7* and *Tlr9* could be explained entirely by the genomic context of these genes. The local GC content was calculated from intronic sequences based on the assumption that any bias in the GC content of these sequences primarily reflects nonselective effects of genomic context. Our analysis confirmed a correlation between intronic GC content and CAI (Spearman R^2: human = 0.61, mouse = 0.45) (Fig. 1*B*). Accordingly, *Tlr7* and *Tlr9* fell along this axis, suggesting that a large portion of the codon bias observed in these genes is explained by the local GC content.

We also wondered if we could detect selection for codon bias toward either poor or favored codons by comparison with genes in similar chromosomal contexts. We performed further analyses of the CAI taking into account the local GC content of all intron-containing CDS. Comparison with genes with similar (within 2.5%) GC content revealed that, even after accounting for chromosomal

context, *Tlr7* still reflected a codon bias toward infrequent codons (mouse: seventh percentile; human: 17th percentile), whereas *Tlr9* displayed less of a bias (mouse: 55th percentile; human: 68th percentile) (Fig. 1*B*). Thus, although local GC content can explain the majority of the codon use, there is evidence of evolutionary pressure to maintain suboptimal codons in the coding region of *Tlr7* at a higher frequency than would be expected for its chromosomal context; the optimal codons used by *Tlr9* may simply reflect the GC content of its chromosomal context.

Based on the different CAI scores for *Tlr7* and *Tlr9*, we looked for differences in the use of specific codons representative of differences in codon bias between *Tlr7* and *Tlr9*. We reasoned that leucine codon use may be significant, given the relative abundance of leucine in TLR genes, a result of the leucine-rich repeats within TLR ectodomains. Strikingly, murine *Tlr7* and *Tlr9* varied in their use of almost all leucine-encoding codons (Fig. 1*C*). Most dramatic was the difference in their use of the frequently used CTG and infrequently used TTA codons. CTG is present in the *Tlr7* CDS 18.6% of the time (31/167), less than half of the 39.6% genome-wide average, whereas CTG is used 56.0% of the time (107/191) in *Tlr9* CDS. TTA use in *Tlr7* CDS is almost twice the genomic average (14.4% vs. 7.5%, 24/167), but TTA is used only once (0.5%) in the *Tlr9* CDS. Thus, although TLR7 and TLR9 are closely related proteins, *Tlr7* has an inherent bias toward infrequent codons within its coding region, particularly in its use of the codons encoding leucine.

Codon Optimization of *Tlr7* Affects Protein Production in a Heterologous System. To address the relevance of the differential codon bias in *Tlr7* and *Tlr9*, we compared the expression of epitope-tagged proteins in a heterologous system. We used the Flp-In T-REx 293 system, which integrates a single copy of a transgene into a fixed genomic location under the control of a doxycycline-inducible CMV promoter. This system enables comparisons of expression that are less prone to experimental variations such as transfection efficiency or differences in genomic context. Directly comparing the WT CDS for *Tlr7* and *Tlr9* revealed a greater than 40-fold difference in protein levels when detected with antibodies to the same HA epitope (Fig. 2*A*).

To test whether codon bias is responsible for the difference in TLR7 and TLR9 protein levels, we optimized the *Tlr7* CDS using Invitrogen's codon-optimized (CO) GeneArt algorithm, altering 684 of 1,051 codons (65%). When expressed in the T-REx system, CO-*Tlr7* produced protein levels similar to those produced by the *Tlr9* CDS (Fig. 2*A*). Importantly, this increase in protein resulted in enhanced IL-8 production in response to TLR7 ligands (Fig. 2*B*).

Although fully optimizing CDS certainly increases protein expression in mammalian systems, it is unknown whether more modest coding changes can impact expression in a meaningful way. To investigate the consequences of more modest changes to *Tlr7*'s CDS, we focused on codons encoding for leucine because their use is so different between *Tlr7* and *Tlr9* (Fig. 1*C*). Replacing all 105 TTA, TTG, CTT, and CTA codons with the codon CTG increased protein by more than 20-fold (leucine-optimized, LO in Fig. 2*A*). A more modest change, replacing only 23 TTA codons with CTG, increased protein by nearly 10-fold (TTA-optimized, TTA in Fig. 2*A*). Importantly, signaling correlated with the increases in protein levels (Fig. 2*B*). Responses to TLR7 ligands also were increased in primary macrophages transduced with retroviruses encoding LO-*Tlr7* (Fig. 2*C*). To rule out a role for UTRs, we generated T-REx lines restoring *Tlr7*'s native 5′ and 3′ UTRs and observed no additional effect on protein levels (Fig. S1). Therefore, because even modest codon changes altered protein expression, these results suggest that codon bias can fine-tune protein expression and may play an important role in the regulation of protein levels.

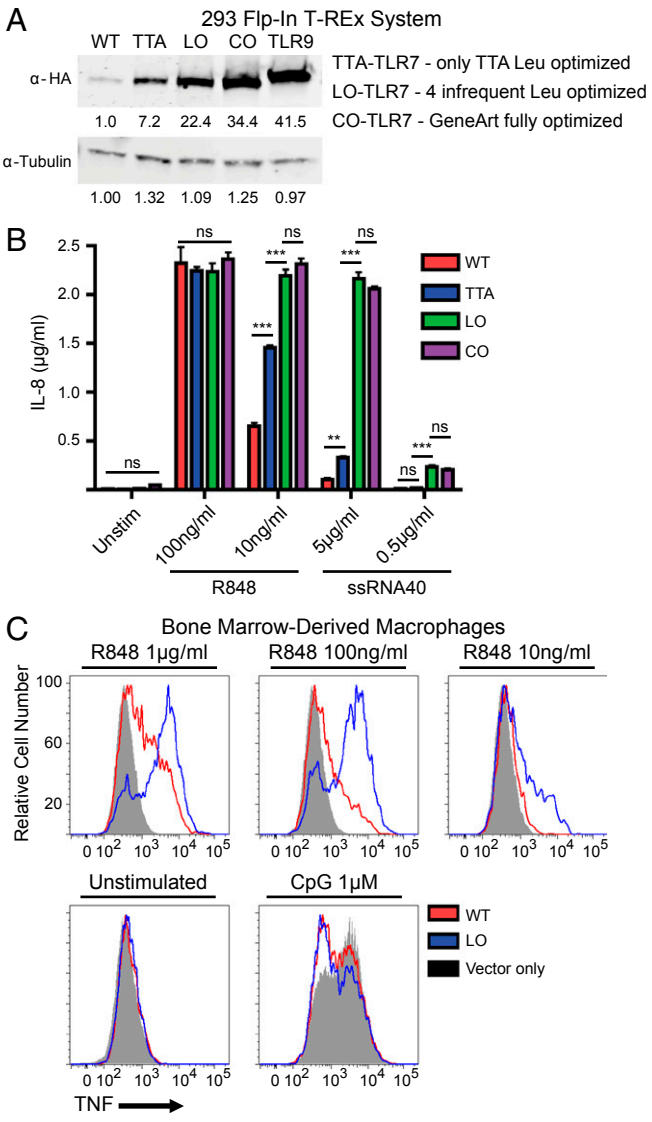

Fig. 2. Codon optimization of *Tlr7* affects protein production in a heterologous system. (*A*) Increased protein expression after codon optimization. *Tlr7* CDS with HA epitope tags were synthesized so that all leucine TTA codons were replaced with CTG (TTA-TLR7); all leucine TTA/TTG/CTT/CTA codons were replaced with CTG (LO-TLR7) or were fully optimized with Invitrogen's GeneArt algorithm (CO-TLR7). These sequences were stably integrated into HEK293 Flp-In T-REx cells. Following 18 h of doxycycline treatment, cells were lysed and analyzed by SDS/PAGE Western blot with the indicated antibodies. (*B*) Signaling is increased in optimized cells lines. T-REx lines were treated with doxycycline overnight and then were stimulated with the indicated TLR7 ligands for 18 h, and supernatants were analyzed for human IL-8 production by ELISA. (*C*) Optimization of *Tlr7* increases signaling in macrophages. Transduced macrophages were stimulated with the TLR7 ligand R848 or the TLR9 ligand CpG at the indicated concentrations, and TNFα production was measured by intracellular cytokine staining. Analysis was limited to transduced cells by gating on tdTomato-positive events. Results in *A* and *C* are representative of at least three independent experiments; data in *B* are shown as the mean ± SEM ($n = 3$). ns, not significant; $^{**}P < 0.01$; $^{***}P < 0.001$.

Codon Optimization of the Endogenous *Tlr7* Gene Does Not Increase Protein Levels. We next assessed whether altering codon use within the endogenous *Tlr7* locus could have similar effects on TLR7 protein levels. To codon optimize the endogenous *Tlr7* gene, we used clustered regularly interspaced short palindromic repeats (CRISPR)/CRISPER-associated protein 9 (Cas9) technology to

facilitate homologous recombination in RAW264.7 cells, a macrophage-like cell line that expresses TLR7. We first replaced exon 3 of *Tlr7*, which encodes all of the TLR7 protein except the initiating methionine, with cDNA encoding the fluorophore tdTomato and confirmed proper integration via Southern blot and loss of responsiveness to the TLR7 ligand R848 (Fig. 3 *A* and *B* and Fig. S2). We then retargeted the locus to replace tdTomato with WT-*Tlr7*, TTA-*Tlr7*, and LO-*Tlr7*. *Tlr7* is located on the X chromosome, and RAW264.7 cells are derived from a male BALB/c mouse; thus, this strategy required targeting only a single locus.

Surprisingly, we observed no changes in protein levels in any of the RAW clones expressing *Tlr7* alleles with varying degrees of codon optimization (Fig. 3*C*). To confirm that the different alleles did not alter TLR7 expression, we compared TLR7-induced TNFα production in the RAW clones; again, we were surprised to observe no significant differences (Fig. 3 *D* and *E*). This discrepancy between endogenous expression in RAW cells and heterologous expression in T-REx cells suggested that the impact of codon optimization may be influenced by additional factors. Therefore, it became critical to elucidate the specific mechanism(s) affected by codon bias to understand how expression can be influenced in these distinct contexts.

***Tlr7* and *Tlr9* mRNAs Are Translated with Different Efficiencies.** To begin to dissect the mechanisms underlying the effects of codon optimization, we first examined whether the differences in protein levels between TLR7 and TLR9 and the increased levels of TLR7 upon codon optimization could be attributed directly to effects on translation. We began by comparing the translation states of endogenous *Tlr7* and *Tlr9* mRNAs. Ribosome profiling measures the translational state of transcripts by quantifying both positional differences in ribosome density and the kinetics of ribosome movement along transcripts. Using a published dataset generated from bone marrow-derived dendritic cells (BMDCs) (30), we calculated the translational efficiency (TE) as the total number of ribosome reads per mRNA transcript (normalized for transcript length) (23). The TE of *Tlr7* was sevenfold lower than that of *Tlr9*, reflective of 15.6-fold more *Tlr7* transcripts but only a 2.1-fold increase in ribosome-associated reads (Fig. 4*A* and Fig. S3). Thus, *Tlr7* mRNA has fewer ribosomes bound to each mRNA than does *Tlr9*.

We also used profiling data from BMDCs treated with harringtonine to infer the kinetics of *Tlr7* and *Tlr9* translation. Harringtonine blocks translation initiation but allows bound ribosomes to translocate normally. By comparing the position of ribosomes in treated and untreated samples, conclusions can be drawn about the rate of translation. In the absence of harringtonine, the distribution of ribosomes along *Tlr7* and *Tlr9* were similar (CHX in Fig. 4*A* and Fig. S3). Following harringtonine treatment, the relative ribosome density shifted to the 3′ end of both *Tlr7* and *Tlr9*, as expected in the absence of new initiation. We did notice greater 3′ skewing for *Tlr7* than for *Tlr9* ("Harr" in Fig. 4*A*; also see Fig. S3). The greater shift does not distinguish between increased run-off from the 5′ end and increased retention on the 3′ end; however, normalizing the ribosome density on *Tlr7* directly to *Tlr9* revealed that a greater fraction of ribosomes remained bound to the 3′ end of *Tlr7* (Fig. 4*B*). This difference suggests that the rate of ribosome translocation on *Tlr9* is fast enough that most ribosomes completed translation during the harringtonine treatment. In contrast, ribosomes on *Tlr7* translocated more slowly and therefore were still present on the 3′ end of *Tlr7* mRNA. No distinct pause sites along *Tlr7* were noted in the untreated samples, but minor stalling sites did appear around base pairs 1,800 and 2,700 following harringtonine treatment. Overall these ribosome-profiling data suggest that the general speed of ribosomes translating *Tlr7* is slower than that of those decoding *Tlr9*.

As an independent confirmation of the different translation states of *Tlr7* and *Tlr9*, we performed polysome profile analysis of RAW264.7 cells. Analysis by quantitative RT-PCR (qPCR) revealed that mRNAs for *Tlr7* and *Tlr9* were distributed differentially across the fractions: Proportionally more *Tlr7* was present in fractions with few ribosomes (Fig. 4 *C*–*E*, black arrow), whereas *Tlr9* was present predominantly in fractions with many ribosomes (Fig. 4 *C*–*E*, gray arrow). Importantly, the CDS lengths for *Tlr7* and *Tlr9* are comparable (3,153 and 3,099 bp, respectively), so differences in mRNA distribution across the gradient reflected differences in ribosome density on each mRNA. When considered

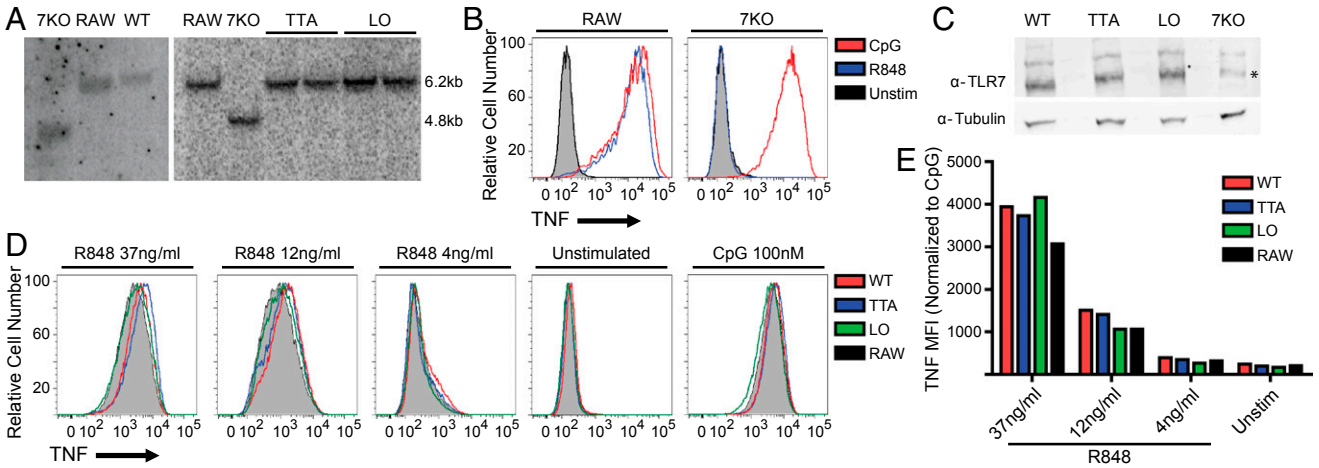

Fig. 3. Codon optimization of the endogenous *Tlr7* locus does not increase protein levels. (*A*) Codon optimization of the endogenous *Tlr7* locus. Proper targeting of the *Tlr7* locus was confirmed by Southern blot analysis. Genomic DNA was digested with NcoI and probed using a region outside of the homology arms. The endogenous fragment is 6.2 kb, whereas proper integration of tdTomato generates a 4.8-kb band. (*Left*) Confirmation of the rescued WT allele. (*Right*) Introduction of codon altered alleles. (*B*) Loss of signaling responsiveness for TLR7. RAW264.7 cell lines were stimulated with the TLR7 ligand R848, and TNFα production was measured by intracellular cytokine staining. (*C*) *Tlr7* alleles in the endogenous locus do not increase protein expression. RAW264.7 cell lines with altered codon biases, as described in *A*, were lysed and analyzed by SDS/PAGE Western blot with the indicated antibodies. The asterisk indicates a nonspecific band that runs just above TLR7. (*D*) *Tlr7* alterations do not increase TNFα production. RAW264.7 cell lines with altered codon biases, as described in *A*, were stimulated with the indicated concentrations of the TLR7 ligand R848 or TLR9 ligand CpG, and TNFα production was measured as in *B*. (*E*) Quantification of geometric mean fluorescent intensity (MFI) in *D* normalized to corresponding CpG mean fluorescent intensity. Results in *C*, *D*, and *E* are representative of three independent experiments.

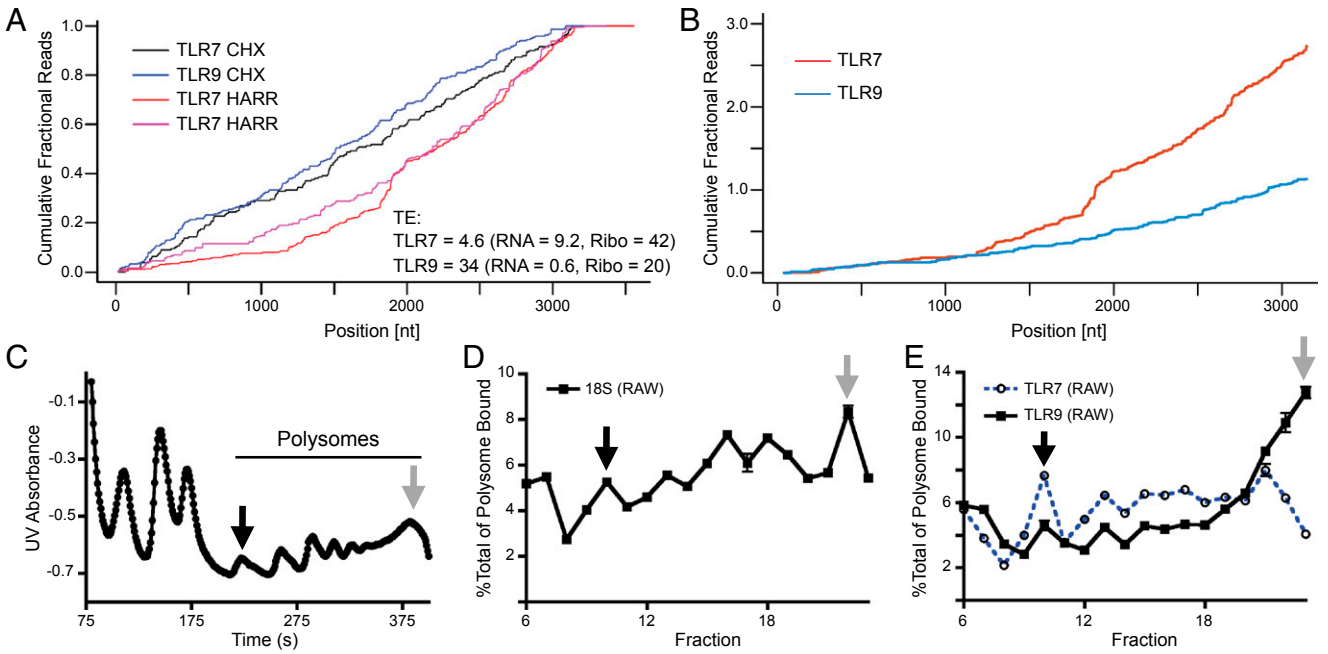

Fig. 4. *Tlr7* and *Tlr9* mRNAs are translated with different efficiencies. (*A*) *Tlr7* and *Tlr9* have different translation efficiencies and behave differently after harringtonine (HARR) treatment. Quantitation of ribosome profiles are presented as the cumulative fraction of reads summed in the 5′ to 3′ direction along the transcript normalized to each gene's total ribosome counts. Translational TE, RNAseq read-count (RNA), and ribosome-associated read-count (Ribo) for the respective transcripts are noted (see *Materials and Methods* for the calculation). CHX, cycloheximide. (*B*) Analysis similar to that in *A*, except that *Tlr7* reads are normalized to *Tlr9*. (*C*) Polysome profile of RAW264.7 cells. Following ultracentrifugation of sucrose gradients, polysomes were fractionated while UV absorbance was monitored. mRNAs containing few ribosomes are in the earlier fractions (black arrow), and mRNAs containing numerous ribosomes are in heavier fractions (gray arrow). (*D*) qPCR of fractions accurately represents the polysome profile. qPCR of ribosomal RNA (18S) in polysome-containing fractions (6–23), normalized to luciferase (spike-in control), and plotted as percent of total polysome-associated 18S RNA. (*E*) *Tlr7* and *Tlr9* have different profiles. qPCR of *Tlr7* and *Tlr9* in polysome-containing fractions, normalized to luciferase and plotted as percent of total respective mRNA bound by polysomes. Results in *C*–*E* are representative of two independent experiments.

together with the ribosome-profiling results described above, these results argue that the translational states for *Tlr7* and *Tlr9* transcripts are distinct and allow for the possibility that codon bias may tune translation efficiency.

Codon Optimization Modestly Affects the Rate of Translation. To determine whether codon optimization of TLR7 affects translation efficiency, we performed polysome profiling of cells expressing codon-optimized versions of *Tlr7*. In the T-REx clone expressing CO-*Tlr7*, most *Tlr7* transcripts were present in the heavier ribosome-dense fractions, similar to the profile of *Tlr9* in RAW cells (compare Figs. 4*E* and 5*A*). The more modest leucine optimization also resulted in a dramatic shift in the polysome profile (Fig. 5*A*). Other transcripts, such as GAPDH, were distributed similarly between the clones, indicating that the global translation state was unaltered.

We also profiled RAW clones expressing either WT-*Tlr7* or LO-*Tlr7* and observed a shift in LO-*Tlr7* message to ribosome-dense fractions, suggesting that the TE of *Tlr7* is altered in these cells (Fig. 5*B*). The shift to dense polysome fractions was less dramatic than in the T-REx lines, perhaps because of differences in translation in the two cell lines. Indeed, the WT-*Tlr7* polysome profiles differed slightly in the T-REx and RAW lines (WT in Fig. 5 *A* and *B*).

Although these profiling data support the conclusion that codon optimization improves TE, we were puzzled that LO-*Tlr7* and CO-*Tlr7* produced such similar polysome profiles (Fig. 5*A*), when clearly less TLR7 protein was detectable in LO-*Tlr7*–expressing cells (Fig. 2*A*), and wondered why the effect of optimization on TE depended on cell type. These discrepancies made us question whether the polysome profiling analyses fully captured the effects of codon optimization. Therefore, to measure the translation of each *Tlr7* mRNA directly, we transfected capped, polyadenylated transcripts of each *Tlr7* variant into HEK293 cells (the parental cell line of the T-REx clones) and measured TLR7 protein 18 h later (Fig. 5*C* and Fig. S4). Although we did observe increased TLR7 protein in cells transfected with TTA-*Tlr7*, LO-*Tlr7*, and CO-*Tlr7* mRNA as compared with cells transfected with WT-*Tlr7* mRNA, the increases were quite modest compared with the increased protein levels in the T-REx clones (compare Figs. 2*A* and 5*C*). Differences between WT-*Tlr7* and *Tlr9* also were less than threefold by this assay. These results suggest that the changes in ribosome occupancy associated with codon bias may have only a minor impact on translation of these mRNAs, accounting for a threefold rather than 30-fold difference in the case of CO-*Tlr7*. In light of these data, we next sought additional mechanistic explanations for the substantial increase in protein levels that we observed in cells expressing codon-optimized TLR7.

Codon Bias Affects mRNA Levels by Altering Transcription. To explain how codon differences between *Tlr7* and *Tlr9* could lead to dramatic differences in protein levels without a major impact on translation, we considered whether codon bias influenced mRNA levels. Previous studies of codon-optimized mammalian proteins have noted a correlation between codon bias and RNA levels. However, there is considerable disagreement as to whether the increase in RNA plays a minor or major role in protein levels and about the mechanisms responsible for the increase (26–29). Strikingly, Northern blot analyses of T-REx clones revealed a large (50-fold) difference in mRNA levels between WT-*Tlr7* and *Tlr9* (Fig. 6*A*), comparable to the overall difference seen at the protein level, and codon optimization increased mRNA levels of CO-*Tlr7* by 42-fold, again closely correlating with changes in protein levels. Importantly, we saw that more modest codon changes in *Tlr7* correlate with more modest increases in RNA levels. These differences

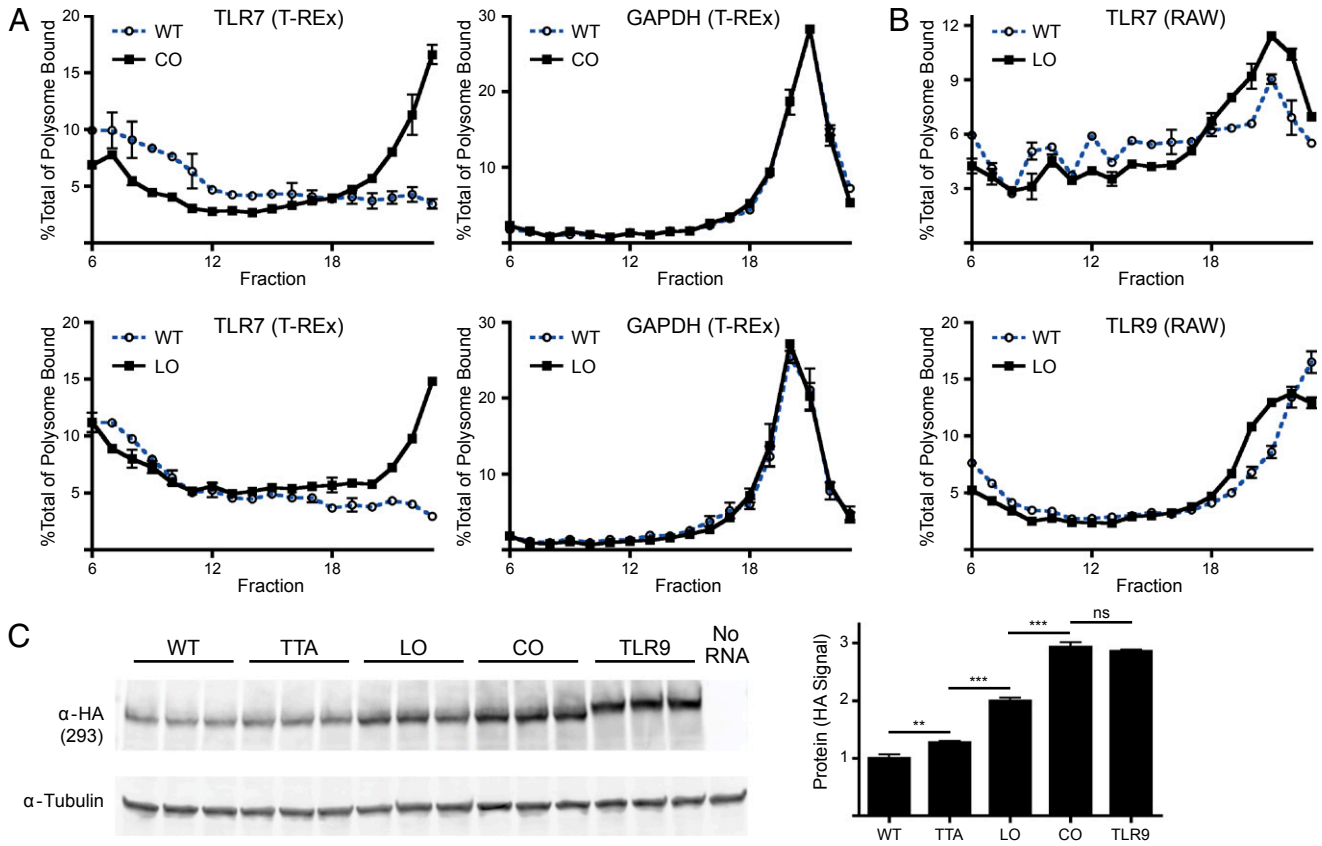

Fig. 5. Codon optimization modestly affects the rate of translation. (*A*) Polysome profiles reveal increased ribosome density upon optimization. Lysates of T-REx lines were analyzed by sucrose gradient ultracentrifugation for WT-*Tlr7* (blue dashed trace) or CO-*Tlr7* (black solid trace). RNA levels were assessed by qPCR for a common 5′ T-REx/*Tlr7* UTR and *Gapdh*. (*B*) Polysome profiles for codon-optimized *Tlr7* in the endogenous locus has only a modest increase in translation efficiency. Lysates of rescued *Tlr7* RAW264.7 lines were analyzed by sucrose gradient ultracentrifugation for WT-*Tlr7* (blue dashed trace) or LO-*Tlr7* (black solid trace). RNA levels were assessed by qPCR for a common *Tlr7* region and *Tlr9*. (*C*) Codon bias modestly alters translation. HEK293 cells were transfected with the mRNAs from Fig. S4 and 18 h later were lysed and analyzed by SDS/PAGE Western blot with the indicated antibodies (*Left*) and were quantified and shown as the mean ± SEM ($n = 3$) (*Right*). Data in *A* and *B* are shown as the mean ± SEM ($n = 2$). The results in *C* are representative of three independent experiments. ns, not significant; $^{**}P < 0.01$; $^{***}P < 0.001$.

are in agreement with reports that codon optimization has a dramatic effect on RNA levels that can account for most of the increase in protein levels (28, 29). However, in contrast to the observations for *Tlr7* transgenes, codon changes in the endogenous coding region of the RAW cells did not result in a significant increase in RNA as assessed by qPCR (Fig. 6*B*). Thus, the discrepancy between the T-REx and RAW systems (i.e., enhanced *Tlr7* levels in the former but not in the latter) can be explained by the differential effect of codon changes on overall RNA levels.

We next explored possible mechanisms that would affect RNA levels caused by codon differences. We first investigated changes in RNA stability, inspired by previous reports which have suggested that codon differences influence transcript stability through translational stalling and no-go decay (NGD) and our finding of possible ribosome stalling along *Tlr7* (Fig. 4*A*) (27). We assessed RNA half-lives by inhibiting transcription in the T-REx clones with actinomycin D and monitoring subsequent RNA levels. *Tlr9* was more stable than WT-*Tlr7*, and fully optimizing the CDS of *Tlr7* improved stability as well (Fig. 6*C*). However, the differences in half-life were less than twofold and were too minor to explain the overall differences in RNA and protein levels. In this assay we could not determine whether the increased stability is caused by decreased stalling and subsequent NGD or by GeneArt's proprietary algorithm being designed to eliminate translation-independent RNA instability motifs. More importantly, the stability of TTA-*Tlr7* and LO-*Tlr7* RNAs was not significantly different from that of WT-*Tlr7*, but both TTA-*Tlr7* and LO-*Tlr7* produced greater *Tlr7* mRNA levels than WT-*Tlr7*. Thus, the effect of codon bias on RNA stability does not adequately explain the changes in RNA levels.

Because RNA stability was largely unaffected, we considered whether codon bias affects transcription, thereby leading to differences in RNA levels. Codon optimization generally increases GC content (Fig. 1*B*), and previous reports have demonstrated a correlation between increased GC content and an increased level of transcription (28, 29), possibly as a result of a decrease in transcriptional pausing (33). We used 4-thiouracil RNA labeling in the T-REx clones to measure the overall rate of transcription. We observed that the rate of transcription was indeed greater for *Tlr9* than for WT-*Tlr7* (Fig. 6*D*). Likewise, fully optimizing codons in *Tlr7* led to a significant increase in the rate of transcription. Importantly, this increase in transcription scaled with the level of optimization. Therefore, in the T-REx system, codon bias directly affected transcription.

To investigate more directly the correlation between increased GC content and increased TLR7 protein levels, we generated another *Tlr7* allele (GC-*Tlr7*) with GC content equivalent to that of LO-*Tlr7* but with codons other than leucine changed. Analysis of T-REx cells expressing GC-*Tlr7* revealed increased protein levels relative to WT TLR7 (Fig. 6*E*). TLR7 protein levels in GC-*Tlr7*–expressing cells did not reach levels equivalent to those of cells expressing LO-*Tlr7*. However, the increase in RNA in the GC-*Tlr7*–expressing cells also was less than in LO-*Tlr7* cells

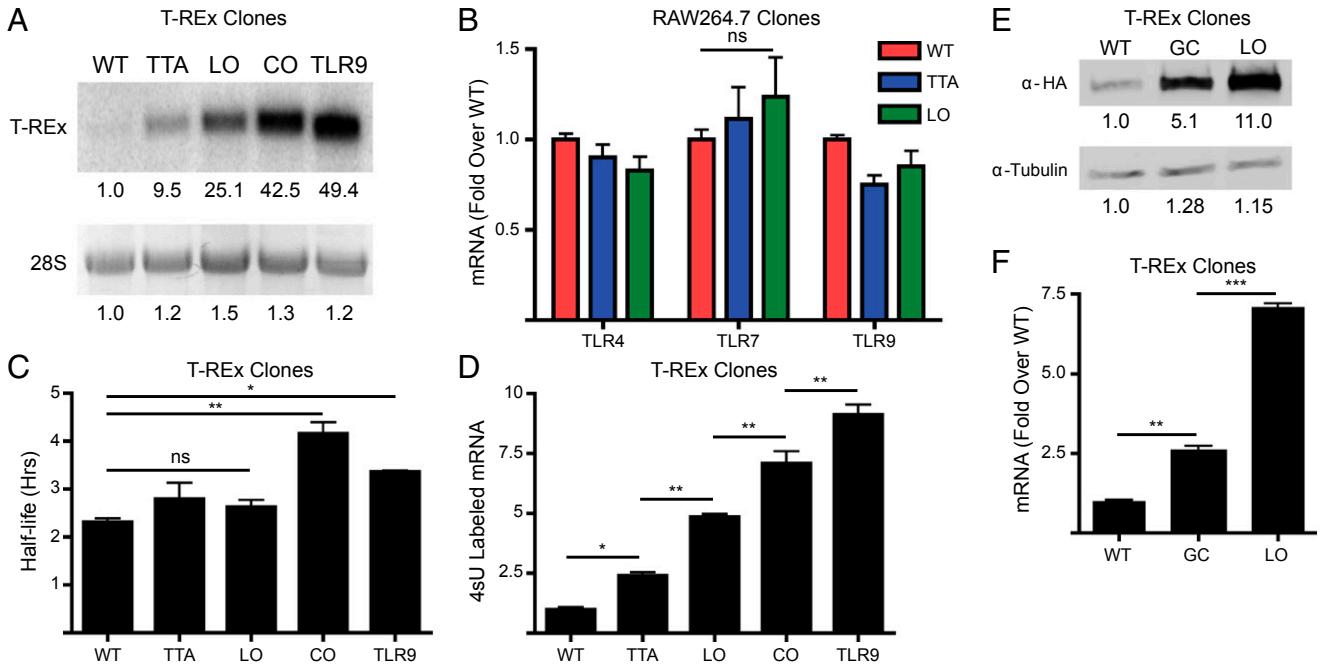

Fig. 6. Codon bias affects mRNA levels by altering transcription. (*A*) mRNA levels differ in T-REx lines. (*Upper*) Northern blot analysis of mRNA levels of T-REx lines treated with doxycycline overnight and probed with the P32-labeled probe common to the 5′ UTR of all mRNAs. (*Lower*) The 28S rRNA band after EtBr staining on a denaturing agarose gel. (*B*) *Tlr7* mRNA expression levels are not altered significantly following optimization of the endogenous *Tlr7* locus. Quantitation was performed using qPCR with normalization to *Gapdh*. (*C*) Minor differences in mRNA stability in T-REx lines. T-REx lines were treated with doxycycline overnight, and total RNA was harvested after actinomycin-D treatment. mRNA levels were assessed by qPCR, normalized to 18S rRNA, and used to calculate half-life. (*D*) The level of transcription differs in T-REx lines. Lines were treated with doxycycline overnight and then were pulsed with 4-thiouracil for 30 min. Total RNA was harvested, labeled with biotin, and pulled down with streptavidin magnetic beads. The eluted RNA was used for cDNA synthesis. Labeled mRNA levels were assessed by qPCR of the common 5′ T-REx UTR normalized to *Gapdh*. (*E*) Altering the GC content alters TLR7 protein levels. T-REx cells expressing WT-*Tlr7*, LO-*Tlr7*, or GC-*Tlr7* were treated with doxycycline for 18 h, lysed, and analyzed by SDS/PAGE Western blot with the indicated antibodies. (*F*) Altering GC content alters TLR7 mRNA levels. T-REx cells expressing WT-*Tlr7*, LO-*Tlr7*, and GC-*Tlr7* were treated with doxycycline for 18 h, and total RNA was harvested. mRNA levels were assessed by qPCR of the common 5′ T-REx UTR normalized to *Gapdh*. Results in *A* and *E* are representative of at least three independent experiments. Data in *B* are shown as the mean ± SEM ($n = 4$), and data in *C*, *D*, and *F* are shown as the mean ± SEM ($n = 2$). Ns, not significant; $*P < 0.05$; $**P < 0.01$; $***P < 0.001$.

(2.6-fold vs. 7.1-fold) (Fig. 6*F*). Thus, as with the other TLR7 alleles, increased GC content correlated with increased RNA and protein levels. The partial effect, relative to LO-*Tlr7*, could be caused by differences between the two alleles in local GC content, which we could not eliminate. Taken together, our results show that although codon optimization can provide a modest improvement in both translation and RNA stability, the most profound effect is an improvement in the overall rate of transcription, likely resulting from the increase in GC content following codon optimization.

Discussion

Our interest in the regulation of TLR7 and TLR9 stems not only from the clear importance of limiting inappropriate responses to self-derived nucleic acids but also from their seemingly paradoxical opposing roles in mouse models of autoimmunity. The balance between these receptors is particularly important in mouse models of SLE (15–17). In this study we investigated the influence of *Tlr7*'s and *Tlr9*'s divergent codon bias on expression. Importantly, we have demonstrated that codon bias can limit expression of TLR7, consistent with the hypothesis that it is important to restrict expression of this receptor. However, the surprising finding we describe here is that the mechanism most affected by codon bias is the overall rate of transcription.

Several groups have attributed the increased protein production following codon optimization predominantly to an increase in translation (26, 27). It should be noted, however, that these studies also observed increased mRNA levels, a point we discuss in greater detail below. Furthermore, a recent study in yeast demonstrated a link among codon bias, translation rate, and RNA stability (34). Thus, codon bias has been suggested to influence several other key mechanisms that regulate protein expression. Of course, these mechanisms potentially affected by codon bias are not mutually exclusive, and, in fact, we do observe changes in translation and RNA stability of *Tlr7* mRNA upon codon optimization. Therefore, an important aspect of our study is the ability to quantify the relative influence of each stage of gene expression on overall protein levels. Analyzing constructs with varying degrees of codon optimization allowed us to separate the influence of more minor mechanisms from the major transcriptional effect. A key role for transcription is particularly supported by our analysis of TTA-*Tlr7*–expressing T-Rex cells, in which we observe an increase in mRNA and subsequent protein levels but no discernable effect on mRNA stability and only a very modest impact on translation of in vitro-transcribed RNA.

Our observation that codon optimization improves protein production primarily by increasing mRNA transcription, likely through alterations in GC content, also may explain why codon optimization of exon 3 within the endogenous *Tlr7* locus does not alter protein production. The endogenous locus contains a 21.5-kb intron between exons 2 and 3 (Fig. S2). Any transcriptional effect arising from alterations in the GC content of the *Tlr7* CDS may be negated by this large intron with relatively low GC content (Fig. 1*B*). In the T-REx system and in retrovirally transduced primary macrophages, the *Tlr7* CDS is expressed without introns. Thus, the discrepancy between the heterologous

and endogenous contexts may be explained by the presence of introns potentially providing an additional dampening effect on the level of transcription and subsequent RNA levels.

The mechanisms that influence the overall rate of transcription are multifaceted and are the subject of intense research, in part because of the advent of improved sequencing technologies. Although initiation and promoter-proximal pausing of RNA polymerase II are generally accepted to be rate-limiting regulatory steps (35), the elongation rate in the body of the transcript also has been shown to correlate with overall mRNA production (36, 37). Of note, a previous study has shown a direct role for GC content in affecting translocating RNA polymerase II by influencing the number and duration of pauses along a transcript (33). Thus, local GC content may influence polymerase activity. This mechanism could explain the difference in RNA levels we observe between the GC-*Tlr7* and LO-*Tlr7* T-REx lines, because we could not precisely match the local GC content between these TLR7 alleles (Fig. 6*F*). Studies similar to ours also have concluded that the predominant effect of altering codon bias in mammalian systems is a change in the overall rate of transcription resulting from changes in GC content (28, 29). However, these reports focused on a limited set of proteins, including the non-mammalian reporter GFP, so the extent to which GC content influences transcription more generally, especially in biologically meaningful contexts, remains an open question. Thus, our finding that GC content correlates with changes in transcription that may help establish the balance between TLR7 and TLR9 provides evidence that this mechanism can be a general form of regulation with profound biological consequences.

GC content also may have additional effects on other mechanisms thought to impact elongation rate, such as chromatin structure, nucleosome density at exon–intron boundaries (38, 39), and splicing (40), although these mechanisms may apply less to our studies using the T-REx transgenic cells and retrovirally transduced primary macrophages in which *Tlr7* transcripts lack introns. It should be noted that a previous study described a negative correlation between elongation rate and GC content (37); however, this analysis was limited to correlations with CpG dinucleotides. From our studies we cannot discriminate between these potential mechanisms affected by altering GC content.

Why control expression at the level of GC content when dynamic regulation can be achieved through promoters and 3′ UTR regulatory elements? In one model, the genomic context, including the GC content, may establish the baseline expression of a gene, and other elements may tune overall mRNA expression levels. Mutations in promoters and 3′ UTRs can change expression of a gene, providing selectable phenotypic differences. Although less plastic than these mechanisms of regulation, genomic context is not fixed. Insertions, especially transposable elements (41), and deletions can alter the genomic context and GC content of a gene. Our findings demonstrate that the relatively minor substitution of 46 nucleotides in TTA-*Tlr7* was sufficient to alter transcription in the context of a 3.5-kb transcript in T-REx cells. Although we detected no impact on mRNA level after substituting 46 or 129 nucleotides in the endogenous 25.6-kb transcript in RAW264.7 cells, we have not ruled out the possibility that a proportionally larger number of substitutions could have an effect. Additionally, despite being closely related, the endogenous transcripts for *Tlr7* and *Tlr9* are 25.6 kb and 4.3 kb, respectively, potentially reflecting key changes in intron structure that have arisen to regulate the two genes differentially. Thus, it is plausible that changes in genomic context and GC content may alter transcription in concert with other regulatory mechanisms.

The relevance of our findings may extend beyond the regulation of TLR7 and TLR9. Most TLRs possess low GC content and score low for CAI overall, as well as relative to genes with similar GC content; in fact, TLR9 is the notable exception (Table S1). Certain TLR family members are constitutively active when overexpressed (42, 43), and chronic or sustained activation of these receptors, whether by microbial or endogenous ligands, may contribute to pathology (44). Thus, the low GC content of these receptors may limit the likelihood of overexpression. It is puzzling that TLR9 is so distinct, especially considering its amino acid similarity to the highly related TLR7 and TLR8. Additional regulatory mechanisms must prevent TLR9 activation, despite higher protein levels. Our findings may have implications for other carefully regulated systems, such as the expression of oncogenes. A previous report found a potential role for codon bias in regulating the various forms of Ras proteins (27). Although the authors concluded that translation was the key mechanism impacted by codon bias, they did note an increase in mRNA when expressing a codon-optimized *Kras* transgene, consistent with a change in transcription. The authors also noted an increase in both protein and mRNA when targeted to the endogenous *KRAS* locus. However, their targeting strategy bypassed the transcription of several large introns whose GC content is relatively poor compared with that of the related *HRAS* gene (Table S1), leaving open the possibility that the genomic context was disrupted also.

Our results do not rule out the possibility that codon bias can influence additional mechanisms beyond transcription. We did see real, although modest, effects on translation and RNA stability. Although we see no evidence that these mechanisms play a role in RAW cells, it is possible that they feature more prominently in other cell types, such as B cells and dendritic cells, where TLR7 regulation is particularly important. The influences of codon bias on translation and RNA stability are less dependent on genomic context, potentially making codon bias a more universal mechanism for regulation. However, our results suggest that transcription is more sensitive than either mRNA stability or translation to changes in GC content, so that a greater number of mutations may be required to alter stability or translation than to alter transcription. In general, our results agree with a recent paper that explored the relative contributions of transcription and translation to protein expression in a global scale and found that changes in transcription explained the majority of expression; however, a subset of genes was shown to be sensitive to changes in translation (30). Thus, the relative importance of transcription, translation, and stability is still an open question and likely may be dependent on the context of each gene.

The importance of regulating TLR7 and TLR9 abundance is underscored by the number of mechanisms implicated in restricting signaling. This study adds to the mechanisms potentially involved and further supports the hypothesis that these two closely related receptors are differentially regulated. Additional exploration of the in vivo consequences of altering this codon bias is still required, as is exploration of other genes, including the other TLRs. Nevertheless, our findings demonstrate that the effect of codon bias and GC content on transcription should be taken into account when investigating the regulation of TLR7 and TLR9.

Materials and Methods

Antibodies and Reagents. Antibodies used in this study were anti-HA (3F10; Roche), anti-tubulin (DM1A; EMD Millipore), Alexa Fluor 680 goat anti-rat IgG H+L (Life Technologies), IRDye 800CW goat anti-mouse (Li-Cor), anti–TNFα-APC (MP6-XT22; eBiosciences), human IL-8 ELISA kit (BioLegend), anti-CD16/32 (2.4G2; UC San Francisco), and anti-TLR7 (726606; R&D Systems). Ligands for stimulation were CpG ODN 1668, R848 (InvivoGen) and ssRNA40/LyoVec (InvivoGen). Primers for used for qPCR were 18s, CATTCGAACGTCTGCCCTAT/CCTGCTGCCTTCCTTGGA; human GAPDH, AGAAGGCTGGGGCTCATTTG/AGGGGCCATCCACAGTCTTC; mouse GAPDH, GAAGGTCGGTGTGAACGGA/GTTAGTGGGGTCTCGCTCCTl T-REx common, GTCAGATCGCCTGGAGACGCC/GGATCCGAGCTCGGTACCAAGC; luciferase, GCGCGGTCGGTAAAGTTGTTCC/GACTTTCCGCCCTTCTTGGCC. Guide RNA target sequences (protospacer adjacent motif in bold) were 5′ TLR7, AGGTGTTTTCGATGTGGACA**CGG;** 3′ TLR7, ACAAAAGCAGCTACTGGTAC**AGG;** tdTomato, ACGGAAGAGACAAGTCGACA**TGG.**

TLR7 Constructs. Optimized versions of TLR7 were synthesized by Invitrogen's GeneArt services and subsequently were subcloned into additional vectors. The fully optimized TLR7 sequence (CO-*Tlr7*) was generated by Invitrogen's GeneArt algorithm for optimized expression in mice.

Cell Culture Lines and Reagents. HEK293 and RAW264.7 cell lines were obtained from American Type Culture Collection (ATCC). The Flp-In T-REx 293 system was purchased from Life Technologies. The Phoenix-E packaging cell line was provided by G. Nolan (Stanford University, Stanford, CA). All cell-culture lines were cultured in DMEM supplemented with 10% (vol/vol) FCS, L-glutamine, penicillin-streptomycin, sodium pyruvate, and Hepes (pH 7.2) (Life Technologies). Cell-culture reagents used were cycloheximide cell culture tested (Sigma-Aldrich), actinomycin D (Sigma), Lipofectamine LTX (Life Technologies), and Lipofectamine 2000 (Life Technologies). For generation of Flp-In T-REx 293 Lines, C-terminally HA-tagged constructs were subcloned into pcDNA5/FRT/TO (Life Technologies) and then cotransfected with pOG44 using Lipofectamine LTX. Individual hygromycin-B (Life Technologies)–resistant colonies were isolated and tested for protein expression after the addition of doxycycline (Sigma). To generate RAW Cas9 Lines, *tdTomato* and *Tlr7* sequences lacking the ATG translation start codon were cloned into pUC19 (Life Technologies) flanked by homology arms derived from the genomic sequence adjacent to exon 3 of *Tlr7* (741 bp upstream, 845 bp downstream). Guide RNAs were designed and synthesized as gBlocks as previously described (45) and then were subcloned into pUC19. Humanized Cas9(D10A)-2xNLS-GFP was a gift from the Doudna laboratory, University of California, Berkeley, CA. RAW264.7 cells were transfected using Lipofectamine LTX with equal amounts the guide RNA plasmid, Cas9 plasmid, and donor template plasmid. For the initial round looking for replacement of *Tlr7* with *tdTomato*, cells were sorted first for Cas9 expression by GFP fluorescence and then for tdTomato fluorescence by FACS (Influx sorter; BD Biosciences). Clones were verified for proper integration by Southern blot analysis and loss of response to the TLR7 ligand R848. Following proper integration of *tdTomato*, the process was repeated with various *Tlr7* donor templates, with the exception that cells were sorted by FACS for loss of tdTomato fluorescence and gain of response to R848.

Polysome Profiling. Cell lines were lysed in buffer (20 mM Tris, 150 mM NaCl, 5 mM $MgCl_2$, 1 mM DTT, 100 μg/mL cycloheximide, 1% Triton X-100, 25 U Turbo DNase, 20 U SUPERase In RNAse inhibitor, pH7.4) and were loaded onto 8–48% sucrose gradients composed of lysis buffer lacking Triton and DNase and generated by mixing on a Gradient Station IP system (BioComp Instruments). Samples were centrifuged at 36,000 rpm in an SW-41 rotor (Beckman Coulter). Fractions were collected every 12 s in 2.0-mL Eppendorf tubes on a Gradient Station while UV absorbance was monitored (Econo UV Monitor; Bio-Rad) and then were spiked with 1 ng Luciferase Control mRNA (Promega). Total RNA was harvested using TRI Reagent LS and 1-Bromo-3-Chloropropane (Sigma), with the modification that after the addition of isopropanol samples were passed over RNA Clean and Concentrator-5 columns (Zymo). For RT-qPCR experiments, cDNA was generated using iScript Reverse Transcription Supermix (Bio-Rad) and then was analyzed using SsoAdvanced SYBR Green reagents (Bio-Rad) on a StepOnePlus Real-Time PCR system (Life Technologies), quantified using the ΔΔCt method, and then normalized to the luciferase spike-in control to account for differences between fractions during purification and cDNA synthesis.

Retroviral Transduction of Bone Marrow-Derived Macrophages. Bone marrow was harvested from *Tlr7*$^{-/-}$ mice (generated by S. Akira, Osaka University, Osaka and provided by K. Fitzgerald, UMass Medical School, Worcester, MA) and was cultured in RPMI-1640 medium supplemented with M-CSF, 10% (vol/vol) FCS, L-glutamine, penicillin-streptomycin, sodium pyruvate, and Hepes (pH 7.2) (Life Technologies). All experiments with mice were performed in accordance with the guidelines of the Animal Care and Use Committee at University of California, Berkeley. Constructs were cloned into a modified MSCV vector which drives expression of the gene of interest as well as a downstream tdTomato fluorophore, the latter driven by an independent PGK promoter. Virus was produced in the Phoenix-E packaging cell line by transfection with Lipofectamine LTX. Four hours after transfection the medium was replaced with bone marrow macrophage medium and was moved to a 32 °C incubator overnight. Viral supernatant was harvested and filtered through a 0.45-μm syringe filter (Thermo Fisher). Bone marrow cells were harvested on day 4 of differentiation, transferred to six-well non–tissue culture-treated plates at a density of 1×10^6 cells/mL in 2 mL of macrophage medium, and spinfected at $1{,}250 \times g$ for 90 min at 32 °C with 1 mL of viral supernatant plus Polybrene. The cells then were kept at 32 °C overnight. Spinfection was repeated the following day with fresh viral supernatant. Cells were harvested the next day with cold PBS and were replated in macrophage medium until day 8–10.

Cell Stimulation Assays. 293 T-REx cells were treated with doxycycline overnight and were stimulated with various ligands. The supernatant was collected after 18 h and was analyzed by ELISA for human IL-8 production. RAW264.7 cells were stimulated with the indicated ligands and analyzed for TNF production by intracellular cytokine staining. Cells were stimulated, and GolgiPlug (BD) was added after 30 min followed by incubation for an additional 5 h. Cells were harvested and stained using Cytofix/Cytoperm (BD) and were analyzed on a LSRFortessa X-20 (BD) with further analysis performed on FlowJo software (FlowJo).

Western Blot Analysis. Cell lysates were prepared with radioimmunoprecipitation assay (RIPA) buffer [25 mM Tris (pH 8.0), 150 mM NaCl, 1% Triton X-100, 1% Na deoxycholate, 0.1% SDS, 4 mM EDTA and supplemented with EDTA-free complete protease inhibitor mixture (Roche)]. Cellular debris was pelleted by centrifugation. Lysates were separated by SDS/PAGE, transferred to an Immobilon-FL membrane (Millipore), and probed using the indicated antibodies. Fluorescence was detected using an Odyssey CLx Infrared Imaging System (LI-COR). All images were processed and quantitated using ImageJ software (NIH).

RNA Analysis. For Northern analysis of T-REx lines, cells were treated overnight with doxycycline and harvested for total RNA using RNAzol RT (Molecular Research Center). Total RNA was run on a NorthernMax denaturing gel (Life Technologies) and transferred with 20× SSC buffer to a Hybond N+ membrane (GE Healthcare). A T-REx probe was generated by PCR using the common T-REx qPCR primers to the 5′ UTR and radiolabeled with P^{32}-dCTP (Perkin-Elmer) and the RadPrime DNA Labeling System (Life Technologies). The membrane was hybridized, washed, exposed to a Phosphor Screen, and detected with a Typhoon Imager (GE Healthcare). Images were processed and quantitated using ImageJ.

For 4-thiouracil labeling, T-REx lines were treated overnight with doxycycline. The next day the medium was replaced with fresh medium containing 0.5 mM 4-thiouracil (Sigma) and doxycycline. After 30 min, total RNA was harvested with RNAzol, labeled with EZ-Link HPDP-Biotin (Thermo Scientific Pierce), captured with streptavidin magnetic beads (Thermo Scientific Pierce), and eluted with 100 mM DTT. cDNA was generated using iScript Reverse Transcription Supermix (Bio-Rad), analyzed using SsoAdvanced SYBR Green reagents (Bio-Rad) on a StepOnePlus Real-Time PCR system (Life Technologies), and quantitated using the ΔΔCt method.

For actinomycin-D RNA stability assays, T-REx lines were treated overnight with doxycycline; then 5 μg/mL actinomycin-D (Sigma) was added for 0, 2.5, or 5 h. Total RNA was harvested with RNAzol. cDNA was generated using iScript Reverse Transcription Supermix (Bio-Rad), analyzed using SsoAdvanced SYBR Green reagents (Bio-Rad) on a StepOnePlus Real-Time PCR system (Life Technologies), and quantitated using the ΔΔCt method using 18S as the reference gene. Log of normalized mRNA quantity versus time was plotted to determine the slope *k*; then half-life was calculated as Ln (2)/Ln(k) in hours.

Statistical Analysis. Probability statistics were calculated with Prism4.0c (GraphPad Software) using one-way ANOVA and the Newman–Keuls multiple comparison post test. Number of replicates (N) refers to independent biological replicates that were processed simultaneously and analyzed. Significance is reported as ns = not significant; $*P < 0.05$; $**P < 0.01$; $***P < 0.001$.

Bioinformatics. Genome-wide analysis of codon use was performed on RefSeq collections of human and mouse CDS (46). Most of our analysis was performed using custom R/Bioconductor code using the Biostrings, GenomicRanges, org.Hs.eg.db, org.Mm.eg.db, BSgenome.Hsapiens.UCSC.hg19, BSgenome.Mmusculus.UCSC.mm10, TxDb.Hsapiens.UCSC.hg19.knownGene, and TxDb.Mmusculus.UCSC.mm10.knownGene packages (47–49). Our code first obtained the human and mouse RefSeq transcript datasets, ignoring transcripts on the "haplotype" and "unplaced" chromosomes. We then extracted intron and ORF sequences, arbitrarily selected a single transcript isoform for each gene symbol, and calculated GC content for sequences of interest. We ignored any extracted ORF sequence whose length was not an even multiple of 3 (e.g., pseudogenes). We trimmed each intron sequence by 10 bp at each end to avoid bias resulting from splice-site preferences and used RepeatMasker intron sequences so that intronic GC content should be a reasonable proxy for GC content in the general genomic neighborhood. We exported ORF sequences and calculated CAI scores (32) using the "cai" algorithm from the EMBOSS suite (50) run locally, with the appropriate codon-use tables for murine or human expression. Our final datasets comprised 19,105 (human) or 20,558 (mouse) genes with a CAI score (Fig. 1*A*); of these we further analyzed 17,880 human and 18,428 mouse intron-containing genes (Fig. 1*B*). Published ribosome profiling and mRNA-Seq data were

analyzed to determine the translational efficiencies of TLR7 and TLR9 using previously published methods (23, 30). Overall translation levels were calculated by counting the number of ribosome footprint fragments mapping to the protein-coding regions of *Tlr7* and *Tlr9*. Transcript abundances were estimated using Cufflinks (51). Translational efficiencies were calculated as the ratio between ribosome footprint levels and mRNA abundance.

In Vitro Translation. TLR constructs were cloned into pcDNA3 vectors containing a T7 promoter. To generate RNA, constructs were linearized, extracted with phenol-chloroform, and used in the mMESSAGE mMACHINE T7 Ultra in vitro RNA transcription kit (Life Technologies), following the manufacturer's protocol for generating polyadenylated transcripts. Synthesized RNA then was transfected into HEK293 cells using Lipofectamine 2000, harvested the next day in RIPA buffer, and analyzed by Western blot using the indicated antibodies. Images were processed and quantitated using ImageJ.

Southern Blot Analysis. Genomic DNA was isolated by isopropanol precipitation of Proteinase K (Thermo Fisher)-digested cells. DNA was digested with restriction enzymes overnight and was separated on a 1% agarose gel. Gels were preincubated in denaturation solution (1.5 M NaCl, 0.5 M NaOH) for 1 h and transferred to a Zeta-Probe GT membrane (Bio-Rad) overnight via capillary action. Blots were washed briefly with neutralization buffer (0.5 M Tris·HCl, 1.5 M NaCl), UV cross-linked with the auto setting on a UV Stratalinker 2400 (Stratagene/Agilent), and placed in prehybridization solution [50% formamide, 5× saline-sodium citrate-potassium phosphate-EDTA (SSCPE) (20× SSCPE; 2.4 M NaCl, 0.3 M Na-citrate, 0.2 M potassium phosphate, 0.02 M EDTA), 5× Denhart's solution, 500 μg/mL sheared salmon sperm DNA, 1% SDS] with rotation overnight at 42 °C. DNA probes were generated as described above and added to the membranes in hybridization solution (50% formamide, 5× SSCPE, 1× Denhart's solution, 100 μg/mL sheared salmon sperm DNA, 20% dextran sulfate, 1% SDS). The membrane was washed in 2× SSC three times at 65 °C, exposed to a phosphor screen, and detected with a Typhoon Imager (GE Healthcare). Images were processed and quantitated using ImageJ.

ACKNOWLEDGMENTS. We thank members of the G.M.B. and Vance laboratories for helpful discussions and advice; Hector Nolla and Alma Valeros for assistance with cell sorting at the Cytometry Facility of the Cancer Research Laboratory at the University of California, Berkeley; the Doudna laboratory for CRISPR/Cas9 reagents; and the Weismann laboratory for help with the ribosome profiling analysis. Z.R.N. and G.M.B. were supported by NIH Grants AI072429, AI063302, and AI105184 and by the Lupus Research Institute. J.M.Y. was supported by a grant to Harmit Malik from the Lupus Research Institute and NIH Grant P50 GM107632 (principal investigator: Jef Boeke, New York University). N.T.I. was supported by Searle Scholars Program Grant 11-SSP-229 and by NIH New Innovator Award DP2 CA195768.

1. Marshak-Rothstein A (2006) Toll-like receptors in systemic autoimmune disease. *Nat Rev Immunol* 6(11):823–835.
2. Barbalat R, Ewald SE, Mouchess ML, Barton GM (2011) Nucleic acid recognition by the innate immune system. *Annu Rev Immunol* 29:185–214.
3. Kadowaki N, et al. (2001) Subsets of human dendritic cell precursors express different toll-like receptors and respond to different microbial antigens. *J Exp Med* 194(6): 863–869.
4. Ewald SE, et al. (2008) The ectodomain of Toll-like receptor 9 is cleaved to generate a functional receptor. *Nature* 456(7222):658–662.
5. Sasai M, Linehan MM, Iwasaki A (2010) Bifurcation of Toll-like receptor 9 signaling by adaptor protein 3. *Science* 329(5998):1530–1534.
6. Lee BL, et al. (2013) UNC93B1 mediates differential trafficking of endosomal TLRs. *eLife* 2(2):e00291.
7. Wang J, et al. (2006) The functional effects of physical interactions among Toll-like receptors 7, 8, and 9. *J Biol Chem* 281(49):37427–37434.
8. Desnues B, et al. (2014) TLR8 on dendritic cells and TLR9 on B cells restrain TLR7-mediated spontaneous autoimmunity in C57BL/6 mice. *Proc Natl Acad Sci USA* 111(4): 1497–1502.
9. Fukui R, et al. (2011) Unc93B1 restricts systemic lethal inflammation by orchestrating Toll-like receptor 7 and 9 trafficking. *Immunity* 35(1):69–81.
10. Kiefer K, Oropallo MA, Cancro MP, Marshak-Rothstein A (2012) Role of type I interferons in the activation of autoreactive B cells. *Immunol Cell Biol* 90(5):498–504.
11. Green NM, et al. (2009) Murine B cell response to TLR7 ligands depends on an IFN-beta feedback loop. *J Immunol* 183(3):1569–1576.
12. Leadbetter EA, et al. (2002) Chromatin-IgG complexes activate B cells by dual engagement of IgM and Toll-like receptors. *Nature* 416(6881):603–607.
13. Christensen SR, et al. (2005) Toll-like receptor 9 controls anti-DNA autoantibody production in murine lupus. *J Exp Med* 202(2):321–331.
14. Lau CM, et al. (2005) RNA-associated autoantigens activate B cells by combined B cell antigen receptor/Toll-like receptor 7 engagement. *J Exp Med* 202(9):1171–1177.
15. Christensen SR, et al. (2006) Toll-like receptor 7 and TLR9 dictate autoantibody specificity and have opposing inflammatory and regulatory roles in a murine model of lupus. *Immunity* 25(3):417–428.
16. Nickerson KM, et al. (2010) TLR9 regulates TLR7- and MyD88-dependent autoantibody production and disease in a murine model of lupus. *J Immunol* 184(4):1840–1848.
17. Deane JA, et al. (2007) Control of toll-like receptor 7 expression is essential to restrict autoimmunity and dendritic cell proliferation. *Immunity* 27(5):801–810.
18. García-Ortiz H, et al. (2010) Association of TLR7 copy number variation with susceptibility to childhood-onset systemic lupus erythematosus in Mexican population. *Ann Rheum Dis* 69(10):1861–1865.
19. Shen N, et al. (2010) Sex-specific association of X-linked Toll-like receptor 7 (TLR7) with male systemic lupus erythematosus. *Proc Natl Acad Sci USA* 107(36):15838–15843.
20. Chamary JV, Parmley JL, Hurst LD (2006) Hearing silence: Non-neutral evolution at synonymous sites in mammals. *Nat Rev Genet* 7(2):98–108.
21. Plotkin JB, Kudla G (2011) Synonymous but not the same: The causes and consequences of codon bias. *Nat Rev Genet* 12(1):32–42.
22. Ingolia NT, Ghaemmaghami S, Newman JRS, Weissman JS (2009) Genome-wide analysis in vivo of translation with nucleotide resolution using ribosome profiling. *Science* 324(5924):218–223.
23. Ingolia NT, Lareau LF, Weissman JS (2011) Ribosome profiling of mouse embryonic stem cells reveals the complexity and dynamics of mammalian proteomes. *Cell* 147(4): 789–802.
24. Tuller T, Waldman YY, Kupiec M, Ruppin E (2010) Translation efficiency is determined by both codon bias and folding energy. *Proc Natl Acad Sci USA* 107(8):3645–3650.
25. Dana A, Tuller T (2012) Determinants of translation elongation speed and ribosomal profiling biases in mouse embryonic stem cells. *PLOS Comput Biol* 8(11):e1002755.
26. Robinson F, Jackson RJ, Smith CWJ (2008) Expression of human nPTB is limited by extreme suboptimal codon content. *PLoS One* 3(3):e1801.
27. Lampson BL, et al. (2013) Rare codons regulate KRas oncogenesis. *Curr Biol* 23(1): 70–75.
28. Kudla G, Lipinski L, Caffin F, Helwak A, Zylicz M (2006) High guanine and cytosine content increases mRNA levels in mammalian cells. *PLoS Biol* 4(6):0933–0942.
29. Bauer AP, et al. (2010) The impact of intragenic CpG content on gene expression. *Nucleic Acids Res* 38(12):3891–3908.
30. Jovanovic M, et al. (2015) Dynamic profiling of the protein life cycle in response to pathogens. *Science* 347(6226):1259038.
31. Zhong F, et al. (2005) Deviation from major codons in the Toll-like receptor genes is associated with low Toll-like receptor expression. *Immunology* 114(1):83–93.
32. Sharp PM, Li WH (1987) The codon Adaptation Index–a measure of directional synonymous codon usage bias, and its potential applications. *Nucleic Acids Res* 15(3): 1281–1295.
33. Zamft B, Bintu L, Ishibashi T, Bustamante C (2012) Nascent RNA structure modulates the transcriptional dynamics of RNA polymerases. *Proc Natl Acad Sci USA* 109(23): 8948–8953.
34. Presnyak V, et al. (2015) Codon optimality is a major determinant of mRNA stability. *Cell* 160(6):1111–1124.
35. Jonkers I, Lis JT (2015) Getting up to speed with transcription elongation by RNA polymerase II. *Nat Rev Mol Cell Biol* 16(3):167–177.
36. Danko CG, et al. (2013) Signaling pathways differentially affect RNA polymerase II initiation, pausing, and elongation rate in cells. *Mol Cell* 50(2):212–222.
37. Jonkers I, Kwak H, Lis JT (2014) Genome-wide dynamics of Pol II elongation and its interplay with promoter proximal pausing, chromatin, and exons. *eLife* 3(3):e02407.
38. Tilgner H, et al. (2009) Nucleosome positioning as a determinant of exon recognition. *Nat Struct Mol Biol* 16(9):996–1001.
39. Schwartz S, Meshorer E, Ast G (2009) Chromatin organization marks exon-intron structure. *Nat Struct Mol Biol* 16(9):990–995.
40. Amit M, et al. (2012) Differential GC content between exons and introns establishes distinct strategies of splice-site recognition. *Cell Reports* 1(5):543–556.
41. Cowley M, Oakey RJ (2013) Transposable elements re-wire and fine-tune the transcriptome. *PLoS Genet* 9(1):e1003234.
42. Fitzgerald KA, et al. (2001) Mal (MyD88-adapter-like) is required for Toll-like receptor-4 signal transduction. *Nature* 413(6851):78–83.
43. Ozinsky A, et al. (2000) The repertoire for pattern recognition of pathogens by the innate immune system is defined by cooperation between toll-like receptors. *Proc Natl Acad Sci USA* 97(25):13766–13771.
44. Kondo T, Kawai T, Akira S (2012) Dissecting negative regulation of Toll-like receptor signaling. *Trends Immunol* 33(9):449–458.
45. Mali P, et al. (2013) RNA-guided human genome engineering via Cas9. *Science* 339(6121):823–826.
46. Pruitt KD, et al. (2014) RefSeq: An update on mammalian reference sequences. *Nucleic Acids Res* 42(Database issue, D1):D756–D763.
47. R Core Team (2014) R: A language and environment for statistical computing. Available at https://www.r-project.org/. Accessed June 1, 2015.
48. Gentleman RC, et al. (2004) Bioconductor: Open software development for computational biology and bioinformatics. *Genome Biol* 5(10):R80.
49. Lawrence M, et al. (2013) Software for computing and annotating genomic ranges. *PLOS Comput Biol* 9(8):e1003118.
50. Rice P, Longden I, Bleasby A (2000) EMBOSS: The European Molecular Biology Open Software Suite. *Trends Genet* 16(6):276–277.
51. Trapnell C, et al. (2012) Differential gene and transcript expression analysis of RNA-seq experiments with TopHat and Cufflinks. *Nat Protoc* 7(3):562–578.